Experimentally Engineering the Edge Termination of Graphene Nanoribbons

Xiaowei Zhang,[†,‡,¶] Oleg V. Yazyev,[†,‡,§,¶] Juanjuan Feng,[†,⊥,¶] Liming Xie,[∥,¶] Chenggang Tao,[†,‡] Yen-Chia Chen,[†,‡] Liying Jiao,[∥] Zahra Pedramrazi,[†] Alex Zettl,[†,‡] Steven G. Louie,[†,‡] Hongjie Dai,[∥] and Michael F. Crommie[†,‡,*]

[†]Department of Physics, University of California at Berkeley, Berkeley, California 94720, United States, [‡]Materials Science Division, Lawrence Berkeley National Laboratory, Berkeley, California 94720, United States, [§]Institute of Theoretical Physics, Ecole Polytechnique Fédérale de Lausanne (EPFL), CH-1015 Lausanne, Switzerland, [⊥]School of Physical Science and Technology, Lanzhou University, Lanzhou, Gansu 730000, China, and [∥]Department of Chemistry and Laboratory for Advanced Materials, Stanford University, Stanford, California 94305, United States. [¶]These authors contributed equally to this work.

ABSTRACT The edges of graphene nanoribbons (GNRs) have attracted much interest due to their potentially strong influence on GNR electronic and magnetic properties. Here we report the ability to engineer the microscopic edge termination of high-quality GNRs *via* hydrogen plasma etching. Using a combination of high-resolution scanning tunneling microscopy and first-principles calculations, we have determined the exact atomic structure of plasma-etched GNR edges and established the chemical nature of terminating functional groups for zigzag, armchair, and chiral edge orientations. We find that the edges of hydrogen-plasma-etched GNRs are generally flat, free of structural reconstructions, and terminated by hydrogen atoms with no rehybridization of the outermost carbon edge atoms. Both zigzag and chiral edges show the presence of edge states.

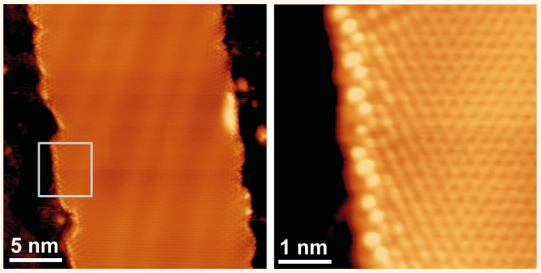

KEYWORDS: graphene nanoribbon · synthesis · scanning tunneling microscopy · first-principles calculations

The edges of graphene exhibit several unique features, such as the presence of localized edge states, and are anticipated to provide an important means of controlling the electronic properties of this two-dimensional material.[1−3] In particular, edges oriented along the high-symmetry zigzag direction or along any low-symmetry (chiral) direction give rise to unique localized edge states[4−9] that are predicted to result in magnetic ordering.[1−3] Such edge-dependent behavior is expected to be even more pronounced in ultranarrow strips of graphene, dubbed nanoribbons, where edges make up an appreciable fraction of the total nanostructure volume, thus creating new nanotechnology opportunities regarding novel electronic and magnetic nanodevices.[2,3] Edge states in chiral nanoribbons have been experimentally observed,[10,11] but it has so far not been possible to control and correlate nanoribbon edge electronic structure with specific chemically defined terminal edge groups.

Here we report a scanning tunneling microscopy (STM) study of graphene nanoribbons (GNRs) that are treated by hydrogen plasma etching. We find that hydrogen plasma etches away the original edge groups and develops segments with different chiralities along the edge. We have closely examined three different types of representative GNR edge segments: zigzag segments, (2,1) chiral edge segments, and armchair segments. Comparison between our experimental data and first-principles simulations of energetically most favorable structures shows good agreement. For example, we find that the edge carbon atoms of our etched GNRs are terminated by only one hydrogen atom, and that both zigzag and chiral edges show the presence of edge states. The edges of hydrogen-plasma-etched GNRs are seen to be generally free of structural reconstructions and curvature,[10,11] with the outermost carbon edge atoms being in the sp^2 hybridization state. Hydrogen plasma etching thus enables the engineering of GNR edges from an unknown terminal group (with associated edge curvature[10,11]) to a flat edge morphology with known atomic termination and terminal bonding symmetry.

* Address correspondence to crommie@berkeley.edu.

Received for review August 16, 2012 and accepted November 29, 2012.

Published online November 29, 2012
10.1021/nn303730v

RESULTS AND DISCUSSION

The investigated GNRs were obtained by hydrogen plasma treatment[12] of chemically unzipped carbon nanotubes[13] deposited onto a Au(111) substrate (see the Methods section). Prior to hydrogen plasma treatment, these GNRs typically exhibit curved edges[10,11,14] that hinder access *via* STM to the very outermost edge atoms. The chemical nature of the pre-etched outermost atoms is therefore unknown, but based on the GNR chemical treatment, they are likely terminated with some form of oxygen-containing functional groups.[10] Figure 1a shows a typical room temperature STM image of a GNR that has been deposited onto Au(111) before being etched by hydrogen plasma. The line profile indicates typical edge curvature, where the curved part of the edge has a width of 5 nm and a height of 0.3 nm above the center terrace region of the GNR.

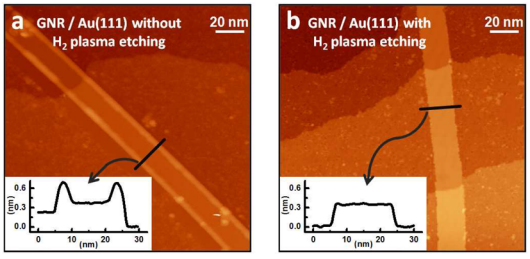

Figure 1. Effect of hydrogen plasma treatment on GNRs deposited on a Au(111) substrate. (a) Room temperature constant-current STM topograph (V_S = 1.5 V, I_t = 100 pA) of a GNR before hydrogen plasma etching. (b) Room temperature STM image of a GNR after hydrogen plasma treatment (V_S = −1.97 V, I_t = 50 pA). Insets show the indicated line profiles.

The effect of hydrogen plasma treatment on these GNRs is two-fold. First, the hydrogen plasma etches away the original edge groups and substitutes them with hydrogen (the simplest possible monovalent edge termination). Second, the edges become significantly rougher and develop short segments (several nanometers long) that display different chiralities within the same GNR (Figures 1b and 2a−e) (the entire GNR thus does not achieve global thermodynamic equilibrium that would result in an overall preferred edge orientation). The combination of these two factors changes the interaction between the edges and the substrate, resulting in a flat, uncurved morphology with the outermost edge atoms being more exposed. Figure 1b shows that the bright strips due to edge curvature are no longer visible in etched GNRs. Instead, the etched GNRs are flat, with a height similar to the height of the interior terrace of unetched GNRs, indicating that the etching process starts from the edges and moves toward the center.

Higher resolution topographic images (Figure 2a−e) on different parts of an etched GNR show the honeycomb structure of the interior graphene. By superimposing a hexagonal lattice structure, we are able to identify the chirality of each segment of the GNR edge (see Supporting Information). Figure 2c−e shows close-up images of three different types of representative GNR edge segments: a zigzag segment, a chiral edge segment orientated along the (2,1) vector of the graphene lattice, and an armchair segment, respectively. The 2 nm long zigzag edge segment (Figure 2c) appears as a sequence of bright spots visible along the edge, which then decays into the interior graphene.

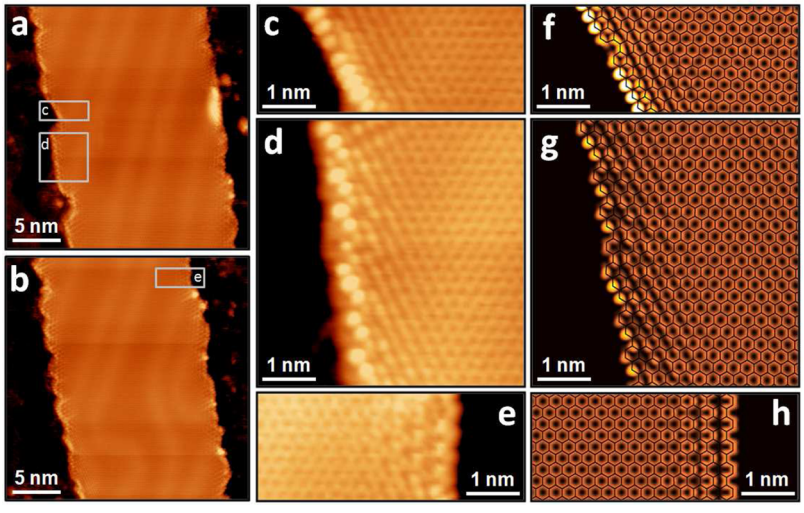

Figure 2. Atomically resolved STM topographs of GNR edges: experiment *vs* first-principles simulations. (a,b) Larger-scale room temperature STM topographs of two segments of a GNR (V_S = −0.97 V, I_t = 50 pA). (c−e) Zoomed-in atomically resolved images of edge segments circled in panels a and b having different chiralities: a zigzag edge (V_S = −0.97 V, I_t = 50), a (2,1) chiral edge (V_S = −0.97 V, I_t = 50 pA), and an armchair edge (V_S = −0.97 V, I_t = 50 pA), respectively. (f−h) STM images simulated from first principles using the Tersoff−Hamann approximation for the STM tunneling current, the same bias voltage as in the experiments, and the thermodynamically most stable hydrogen edge configuration. These simulations suggest that the plasma treatment results in simple edge termination with one hydrogen atom saturating each dangling bond. The atomic structures of the underlying lattices of carbon atoms are shown as black lines.

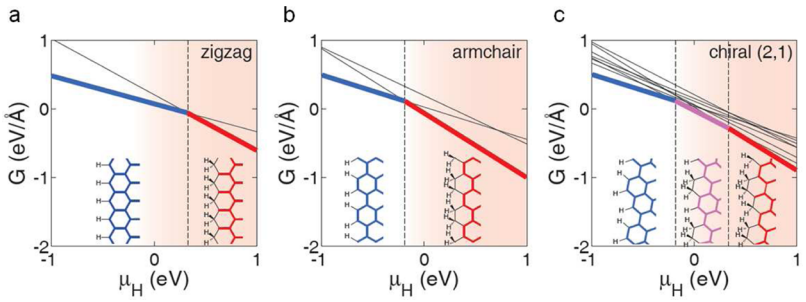

Figure 3. Thermodynamic stability of hydrogenated graphene edges calculated from first principles. Edge formation energy per unit length (G) as a function of chemical potential of hydrogen (μ_H) calculated from first principles for various hydrogen termination patterns for (a) a zigzag, (b) an armchair, and (c) a (2,1) chiral edge of a GNR. The structures for stable edge terminations are sketched below. The sp^2 carbon atom bonding networks are highlighted in color (matched to the energy plot), while sp^3 carbon atoms and terminating bonds are shown in black. The shaded areas denote the range of chemical potentials μ_H for which graphane is more stable than graphene.

This segment exhibits a small depression near the middle of the outer row of edge atoms, while the second row of edge atoms next to the depression appears to be brighter than adjacent second row atoms. The (2,1) chiral edge segment (Figure 2d) shows a periodic modulation in STM intensity along its length. Comparison with a superimposed lattice structure (see Supporting Information) shows that the periodic bright spots are localized along zigzag-like fragments. A break in the periodic pattern is observed in the middle of the chiral edge, possibly due to the presence of a vacancy defect. The armchair edge (Figure 2e), in contrast, shows no edge enhancement in the STM intensity. Instead, the armchair edge exhibits a pronounced standing-wave feature with a periodicity of ~0.4 nm at the −0.97 V bias voltage used in our measurements.

Because the experiments were carried out at room temperature (see the Methods section), thermal effects limit our ability to perform highly resolved STM spectroscopy. Nevertheless, our STM images contain a significant amount of information regarding GNR edge electronic structure. In order to understand this information, we must first determine the bonding arrangement of hydrogen atoms at the GNR edges. Once we know this bonding arrangement, we can then calculate the GNR electronic local density of states and compare it to the STM data to self-consistently confirm the structural model and electronic behavior. Our strategy for performing this procedure is to first calculate the energetic stability of different edge structures and then to use the thermodynamically favorable structures to guide our first-principles electronic property calculations which are then compared to experiment.

We determined the thermodynamically most favorable structures by calculating the edge formation energy of different hydrogen-bonded GNR edge structures in contact with a reservoir of hydrogen. Edge carbon atoms were allowed to terminate with either one (sp^2 hybridization) or two (sp^3 hybridization) hydrogen atoms, and we restricted our consideration only to structural terminations having the same periodicity as the unterminated bare edge since such symmetry is observed experimentally. Different hydrogenated edge structures differ in their local chemical composition, and thus their formation energies per edge unit length depend on the chemical potential of hydrogen, μ_H, according to[15]

$$G(\mu_H) = \frac{1}{2a}\left(E_{GNR} - \frac{N_C}{2}E_{graphene} - \frac{N_H}{2}E_{H_2} - N_H\mu_H\right)$$

where a is the edge periodicity, N_C and N_H are the number of carbon and hydrogen atoms per unit cell, and E_{GNR} and $E_{graphene}$ are the total energies of the model GNR and ideal graphene per unit cell, respectively. The chemical potential, μ_H, here defined using the total energy E_{H_2} of a H_2 molecule as a reference, is a free parameter which depends on particular experimental conditions. For this reason, we analyzed a broad range of chemical potentials, as shown in Figure 3. Structures having the lowest formation energies, $G(\mu_H)$, at a given μ_H are highlighted with thick lines, and the corresponding structures are shown below with the π bonding network emphasized. We note that more stable structures with long-range periodicity can, in principle, be realized,[16] but they are not observed here since global thermodynamic equilibrium is not achieved under the present experimental conditions.

For the zigzag edge (Figure 3a), two hydrogen configurations are possible—either a "simple" sp^2-bonded hydrogen zigzag edge for $\mu_H < 0.33$ eV or an sp^3-bonded edge with two hydrogen atoms per carbon edge atom for $\mu_H > 0.33$ eV (the latter results in the Klein edge π bonding network topology[17]). The shaded region in Figure 3 shows the condition for graphene to transform into graphane[18,19] with a full basal hydrogenation of stoichiometry CH ($\mu_H > -0.2$ eV). Since this is not observed experimentally, meaning $\mu_H < -0.2$ eV, we are able to exclude the Klein edge scenario. We thus conclude that the zigzag GNR is terminated with one hydrogen atom per carbon edge atom.

The armchair edge (which has two carbon edge atoms per unit cell) can, in principle, support three possible hydrogen terminations. As shown in Figure 3b, however,

only two of them have regions of stability—either both carbon edge atoms terminated with one hydrogen atom ($\mu_H < -0.19$ eV) or both carbon edge atoms terminated with two hydrogen atoms ($\mu_H > -0.19$ eV). These two configurations are equivalent from the point of view of the π electron system topology, and both have an identical electronic structure that is consistent with the experimental observation. However, the condition of observing graphene instead of graphane requires $\mu_H < -0.2$ eV, thus indicating that the armchair edge is most likely terminated with one hydrogen atom per carbon atom.

The situation is somewhat more complicated for the case of the (2,1) chiral edge, which has three inequivalent edge atoms per unit cell and thus can realize, in principle, eight distinct possible hydrogen terminations. Only three of these, however, have regions of stability (Figure 3c): the case where all edge atoms are terminated with one hydrogen atom ($\mu_H < -0.19$ eV), the case where two adjacent edge atoms are terminated with two hydrogen atoms and the third edge atom is bonded only to one hydrogen (-0.19 eV $< \mu_H < 0.33$ eV), and the case where all three edge atoms are each terminated with two hydrogen atoms ($\mu_H > 0.33$ eV). The first two structures realize the same π electron network topology. However, because the upper limit of μ_H realized under the present experimental condition is -0.2 eV, we conclude that the (2,1) chiral edge termination should involve only one hydrogen atom per edge carbon atom. This chiral edge termination is equivalent to the previously used models of refs 10 and 20.

To further confirm that the calculated thermodynamically favorable edge terminations correspond to what we observe experimentally, we performed first-principles simulations (see the Methods section) of the STM images for these structures (Figure 2f–h) and compared them to our experimental data. The structural models were based on the energetically most stable termination (*i.e.*, one hydrogen atom per edge carbon atom) and did not involve any covalent bonding reconstructions other than six-membered rings. We did not include the Au(111) substrate in our calculations since Au does not have a significant effect on the overall electronic structure of graphene.[21]

The resulting simulated STM images nicely match the experimental data. This can be seen first for the zigzag segment in Figure 2f, which shows a sequence of bright spots along the edge. A single carbon atom was removed from the center of the zigzag edge in the simulation, and this is seen to explain the depression in the middle of the outer row of atoms and the slight enhancement in the second row of carbon atoms. The simulation of the (2,1) chiral edge (Figure 2g) shows very pronounced edge states in agreement with the experimental data. It also features the observed intensity modulation along the length of this edge, which results from edge states localized along the zigzag-like fragments. An extra pair of edge carbon atoms was added to the middle of this edge segment which effectively elongates one of the zigzag-like fragments and shortens the neighboring one, thus explaining a break in the periodic pattern observed in the middle of the experimental edge segment. The simulated armchair segment (Figure 2h) does not show intensity enhancement along the edge, as seen experimentally for this structure. This is consistent with the fact that this edge orientation does not give rise to localized states (this is further confirmed by average line scans shown in the Supporting Information). The armchair edge simulation also features a standing-wave pattern, in agreement with previously reported predictions[22,23] and the experimental data of Figure 2e. Other possible edge terminations were also simulated for these different edge orientations (see Supporting Information), but they did not reproduce the experimental results nearly as well as those shown. This in-depth experiment/theory comparison provides confirmation that the experimentally observed edge terminations match the theoretically derived most stable hydrogen configurations.

CONCLUSIONS

We have investigated hydrogen-plasma-treated GNRs on a Au(111) substrate. We find that hydrogen plasma etches away unknown edge terminal groups and promotes formation of short segments having different chiralities along the edge. From more than 20 GNRs examined in this study, we observed no apparent preferred orientation of the edge segments. The chirality of edge segments likely has some dependence on the initial chirality of the whole GNR, local environments, and the out-of-equilibrium nature of the hydrogen plasma etching; thus thermodynamics is expected to play only a minor role in determining the overall statistics of edge orientations. We have primarily studied three types of GNR edge segments: zigzag segments, (2,1) chiral edge segments, and armchair segments. Our combination of local probe microscopy and *ab initio* simulations enables us to determine both the terminal hydrogen-bonding structure and the edge electronic structure for edge-engineered graphene nanoribbons. This work has important implications for graphene research and technology as it introduces a new method for controlling the chemical termination and direction of GNR edges required for manipulating their electronic properties.

METHODS

Experiments. The experiments were performed using an Omicron VT-STM operating at room temperature. The Au(111) substrate was cleaned by standard sputter-annealing procedures in ultrahigh vacuum (UHV) before being transferred *ex situ* for spin-coating of GNRs. The GNRs were chemically

fabricated using carbon nanotube unzipping methods (as in ref 13). The sample was then exposed to hydrogen plasma for 15 min (following the procedures described in ref 12). The sample was then placed back into the UHV chamber where it was annealed up to 500 °C for several hours before being transferred *in situ* for UHV STM measurements.

Calculations. First-principles electronic structure calculations were carried out using the local spin density approximation of density functional theory. The models for the first-principles simulations of STM images are approximately 7 nm wide graphene nanoribbons with hydrogen-terminated edges. These large-scale simulations of STM images have been performed using the SIESTA package[24] and a combination of a double-ζ plus polarization basis set, norm-conserving pseudopotentials,[25] and a mesh cutoff of 200 Ry. The atomic positions have been fully relaxed. The STM intensities were calculated using the Tersoff–Hamann approximation[26] assuming a fixed tip sample distance of 5 au and a negative bias of −0.97 V in accordance with experimental conditions. The stabilities of various edge terminations were investigated using moderate size GNR models of approximately 1.5 nm width and a plane-wave-based computational scheme implemented in the Quantum-ESPRESSO package.[27] In these calculations, we used a combination of ultrasoft pseudopotentials[28] and plane-wave kinetic energy cutoffs of 30 and 300 Ry for wave functions and charge density, respectively.

Conflict of Interest: The authors declare no competing financial interest.

Acknowledgment. Research supported by the Office of Naval Research Multidisciplinary University Research Initiative (MURI) Award No. N00014-09-1-1066 (GNR sample preparation and characterization, thermodynamic stability calculation), by the Director, Office of Science, Office of Basic Energy Sciences of the U.S. Department of Energy under Contract No. DE-AC02-05CH11231 (STM instrumentation development and development of numerical simulation tools), and by National Science Foundation Award No. DMR10-1006184 (calculation of theoretical LDOS). O.V.Y. acknowledges support from the Swiss National Science Foundation Grant No. PP00P2_133552 (development of new techniques for edge simulation). L.X., L.J., and H.D. acknowledge support from Samsung and MARCO MSD (development of nanoribbons synthesis and plasma etching).

Supporting Information Available: Determination of chiralities of GNR segments and location of edge states, simulations of different hydrogen termination for zigzag and (2,1) chiral edges, and comparison of average line scan profiles between experimental images and simulations. This material is available free of charge *via* the Internet at http://pubs.acs.org.

REFERENCES AND NOTES

1. Nakada, K.; Fujita, M.; Dresselhaus, G.; Dresselhaus, M. S. Edge State in Graphene Ribbons: Nanometer Size Effect and Edge Shape Dependence. *Phys. Rev. B* **1996**, *54*, 17954–17961.
2. Son, Y.-W.; Cohen, M. L.; Louie, S. G. Half-Metallic Graphene Nanoribbons. *Nature* **2006**, *444*, 347–349.
3. Yazyev, O. V.; Katsnelson, M. I. Magnetic Correlations at Graphene Edges: Basis for Novel Spintronics Devices. *Phys. Rev. Lett.* **2008**, *100*, 047209.
4. Klusek, Z.; Waqar, Z.; Denisov, E. A.; Kompaniets, T. N.; Makarenko, I. V.; Titkov, A. N.; Bhatti, A. S. Observations of Local Electron States on the Edges of the Circular Pits on Hydrogen-Etched Graphite Surface by Scanning Tunneling Spectroscopy. *Appl. Surf. Sci.* **2000**, *161*, 508–514.
5. Kobayashi, Y.; Fukui, K.; Enoki, T.; Kusakabe, K.; Kaburagi, Y. Observation of Zigzag and Armchair Edges of Graphite Using Scanning Tunneling Microscopy and Spectroscopy. *Phys. Rev. B* **2005**, *71*, 193406.
6. Kobayashi, Y.; Fukui, K.; Enoki, T.; Kusakabe, K. Edge State on Hydrogen-Terminated Graphite Edges Investigated by Scanning Tunneling Microscopy. *Phys. Rev. B* **2006**, *73*, 125415.
7. Niimi, Y.; Matsui, T.; Kambara, H.; Tagami, K.; Tsukada, M.; Fukuyama, H. Scanning Tunneling Microscopy and Spectroscopy of the Electronic Local Density of States of Graphite Surfaces near Monoatomic Step Edges. *Phys. Rev. B* **2006**, *73*, 085421.
8. Ritter, K. A.; Lyding, J. W. The Influence of Edge Structure on the Electronic Properties of Graphene Quantum Dots and Nanoribbons. *Nat. Mater.* **2009**, *8*, 235–242.
9. Yang, H.; Mayne, A. J.; Boucherit, M.; Comtet, G.; Dujardin, G.; Kuk, Y. Quantum Interference Channeling at Graphene Edges. *Nano Lett.* **2010**, *10*, 943–947.
10. Tao, C.; Jiao, L.; Yazyev, O. V.; Chen, Y.-C.; Feng, J.; Zhang, X.; Capaz, R. B.; Tour, J. M.; Zettl, A.; Louie, S. G.; *et al.* Spatially Resolving Edge States of Chiral Graphene Nanoribbons. *Nat. Phys.* **2011**, *7*, 616–620.
11. Pan, M.; Girão, E. C.; Jia, X.; Bhaviripudi, S.; Li, Q.; Kong, J.; Meunier, V.; Dresselhaus, M. S. Topographic and Spectroscopic Characterization of Electronic Edge States in CVD Grown Graphene Nanoribbons. *Nano Lett.* **2012**, *12*, 1928–1933.
12. Xie, L.; Jiao, L.; Dai, H. Selective Etching of Graphene Edges by Hydrogen Plasma. *J. Am. Chem. Soc.* **2010**, *132*, 14751–14753.
13. Jiao, L. Y.; Wang, X. R.; Diankov, G.; Wang, H. L.; Dai, H. J. Facile Synthesis of High-Quality Graphene Nanoribbons. *Nat. Nanotechnol.* **2010**, *5*, 321–325.
14. Atamny, F.; Fassler, T. F.; Baiker, A.; Schlogl, R. On the Imaging Mechanism of Monatomic Steps in Graphite. *Appl. Phys. A: Mater. Sci. Process.* **2000**, *71*, 441–447.
15. Qian, G.-X.; Martin, R. M.; Chadi, D. J. First-Principles Study of the Atomic Reconstructions and Energies of Ga- and As-Stabilized GaAs(100) Surfaces. *Phys. Rev. B* **1988**, *38*, 7649–7663.
16. Wassmann, T.; Seitsonen, A. P.; Saitta, A. M.; Lazzeri, M.; Mauri, F. Structure, Stability, Edge States, and Aromaticity of Graphene Ribbons. *Phys. Rev. Lett.* **2008**, *101*, 096402.
17. Klein, D. J.; Bytautas, L. Graphitic Edges and Unpaired pi-Electron Spins. *J. Phys. Chem. A* **1999**, *103*, 5196–5210.
18. Sofo, J. O.; Chaudhari, A. S.; Barber, G. D. Graphane: A Two-Dimensional Hydrocarbon. *Phys. Rev. B* **2007**, *75*, 153401.
19. Elias, D. C.; Nair, R. R.; Mohiuddin, T. M. G.; Morozov, S. V.; Blake, P.; Halsall, M. P.; Ferrari, A. C.; Boukhvalov, D. W.; Katsnelson, M. I.; Geim, A. K.; *et al.* Control of Graphene's Properties by Reversible Hydrogenation: Evidence for Graphane. *Science* **2009**, *323*, 610–613.
20. Yazyev, O. V.; Capaz, R. B.; Louie, S. G. Theory of Magnetic Edge States in Chiral Graphene Nanoribbons. *Phys. Rev. B* **2011**, *84*, 115406.
21. Varykhalov, A.; Sánchez-Barriga, J.; Shikin, A. M.; Biswas, C.; Vescovo, E.; Rybkin, A.; Marchenko, D.; Rader, O. Electronic and Magnetic Properties of Quasifreestanding Graphene on Ni. *Phys. Rev. Lett.* **2008**, *101*, 157601.
22. Wassmann, T.; Seitsonen, A. P.; Saitta, A. M.; Lazzeri, M.; Mauri, F. Clar's Theory, π-Electron Distribution, and Geometry of Graphene Nanoribbons. *J. Am. Chem. Soc.* **2010**, *132*, 3440–3451.
23. Park, C.; Yang, H.; Mayne, A. J.; Dujardin, G.; Seo, S.; Kuk, Y.; Ihm, J.; Kim, G. Formation of Unconventional Standing Waves at Graphene Edges by Valley Mixing and Pseudospin Rotation. *Proc. Natl. Acad. Sci. U.S.A.* **2011**, *108*, 18622–18625.
24. Soler, J. M.; Artacho, E.; Gale, J. D.; Garcia, A.; Junquera, J.; Ordejón, P.; Sánchez-Portal, D. The SIESTA Method for *Ab Initio* Order-N Materials Simulation. *J. Phys.: Condens. Matter* **2002**, *14*, 2745–2779.
25. Troullier, N.; Martins, J. L. Efficient Pseudopotentials for Plane-Wave Calculations. *Phys. Rev. B* **1991**, *43*, 1993–2006.
26. Tersoff, J.; Hamann, D. R. Theory of the Scanning Tunneling Microscope. *Phys. Rev. B* **1985**, *31*, 805–813.
27. Giannozzi, P.; Baroni, S.; Bonini, N.; Calandra, M.; Car, R.; Cavazzoni, C.; Ceresoli, D.; Chiarotti, G. L.; Cococcioni, M.; Dabo, I.; *et al.* QUANTUM ESPRESSO: A Modular and Open-Source Software Project for Quantum Simulations of Materials. *J. Phys.: Condens. Matter* **2009**, *21*, 395502.
28. Vanderbilt, D. Soft Self-Consistent Pseudopotentials in a Generalized Eigenvalue Formalism. *Phys. Rev. B* **1990**, *41*, 7892–7895.